Journal of Translational Medicine

RESEARCH

Open Access

VEGF-A enhances the cytotoxic function of CD4$^+$ cytotoxic T cells via the VEGF-receptor 1/VEGF-receptor 2/AKT/mTOR pathway

Ziyi Chen[1†], Meng Zhang[1†], Yufeng Liu[2,3,4], Zhe Chen[5], Ling Wang[1], Wenjuan Wang[6], Jincheng Wang[6], Mingqian He[1], Bingyin Shi[1*] and Yue Wang[1,2,3*]

Abstract

Background CD4$^+$ cytotoxic T cells (CD4 CTLs) are CD4$^+$ T cells with major histocompatibility complex-II-restricted cytotoxic function. Under pathologic conditions, CD4 CTLs hasten the development of autoimmune disease or viral infection by enhancing cytotoxicity. However, the regulators of the cytotoxicity of CD4 CTLs are not fully understood.

Methods To explore the potential regulators of the cytotoxicity of CD4 CTLs, bulk RNA and single-cell RNA sequencing (scRNA-seq), enzyme-linked immunosorbent assay, flow cytometry, quantitative PCR, and in-vitro stimulation and inhibition assays were performed.

Results In this study, we found that VEGF-A promoted the cytotoxicity of CD4 CTLs through scRNA-seq and flow cytometry. Regarding the specific VEGF receptor (R) involved, VEGF-R1/R2 signaling was activated in CD4 CTLs with increased cytotoxicity, and the VEGF-A effects were inhibited when anti-VEGF-R1/R2 neutralizing antibodies were applied. Mechanistically, VEGF-A treatment activated the AKT/mTOR pathway in CD4 CTLs, and the increases of cytotoxic molecules induced by VEGF-A were significantly reduced when the AKT/mTOR pathway was inhibited.

Conclusion In conclusion, VEGF-A enhances the cytotoxicity of CD4 CTLs through the VEGF-R1/VEGF-R2/AKT/mTOR pathway, providing insights for the development of novel treatments for disorders associated with CD4 CTLs.

Keywords CD4$^+$ cytotoxic T cells, CD4 CTLs, VEGF-A, VEGF-R1, VEGF-R2, mTOR, Graves orbitopathy

†Ziyi Chen and Meng Zhang contributed equally to this work

*Correspondence:
Bingyin Shi
shibingy@126.com
Yue Wang
shelly1021@126.com
[1] Department of Endocrinology, The First Affiliated Hospital of Xi'an Jiaotong University, Xi'an, China
[2] MOE Key Lab for Intelligent Networks & Networks Security, School of Electronic and Information Engineering, Xi'an Jiaotong University, Xi'an, China
[3] Genome Institute, The First Affiliated Hospital of Xi'an Jiaotong University, Xi'an, China
[4] BioBank, The First Affiliated Hospital of Xi'an Jiaotong University, Xi'an, China
[5] Department of Spine Surgery, Hong Hui Hospital, Xi'an Jiaotong University, Xi'an, China
[6] Department of Hematology, The First Affiliated Hospital of Xi'an Jiaotong University, Xi'an, China

Introduction

$CD4^+$ cytotoxic T cells (CD4 CTLs) are $CD4^+$ T cells with major histocompatibility complex (MHC)-II-restricted cytotoxic function possessing a variety of surface markers. Since their discovery in vitro in 1981 and ex vivo in 2004, CD4 CTLs have been reported to be present in both healthy and pathologic conditions [1, 2]. Taniuhi et al. discovered that healthy individuals of all ages (including supercentenarians) had CD4 CTLs in their peripheral blood mononuclear cells (PBMCs) [3]. Additionally, autoimmune diseases, malignancies, and acute and chronic viral infections make up the disorders in which CD4 CTLs play roles [2, 4, 5]. By killing target cells, CD4 CTLs under pathologic conditions, which exhibit upregulated cytotoxic and proinflammatory molecules (e.g., granzyme, perforin, interferon-γ, etc.), are able to control tumor growth and viral infection as well as hasten the progression of autoimmune diseases [6, 7]. Therefore, to better understand the pathogenesis of various diseases and develop novel treatments, it is crucial to investigate the effects and regulatory mechanisms of CD4 CTLs.

Recently, an increasing number of researchers have paid attention to the regulators of the cytotoxicity of CD4 CTLs and revealed that the T cell receptor (TCR), costimulatory/inhibitory molecules and cytokines are potential mediators. Constant exposure to antigens has been shown to enhance the levels of cytotoxic molecules in $CD4^+$ T cells, accompanied by loss of T-helper-inducing POZ/Krueppel-like factor (ThPok, a crucial transcription factor for phenotype maintenance in $CD4^+$ Th cells), which implied a potential role for TCR signaling in the cytotoxicity of CD4 CTLs [8]. Moreover, when agonists specific for the costimulatory molecules CD134 and CD137 were applied in mouse tumor models, eomesodermin (Eomes), which promotes the production of granzyme (Grm)B, was upregulated in CD4 CTLs [9]. Regarding cytokines, IL-15, IL-2, interferon (IFN)-I and IL-18 may enhance the cytotoxic function of CD4 CTLs via the Janus kinase (JAK)/signal transducers and activators of transcription (STAT) pathway [10–12]. However, even after numerous studies have been carried out, the regulators of the cytotoxic function of CD4 CTLs have still not been completely elucidated.

In a previous study, we discovered that CD4 CTLs had elevated cytotoxic function in patients with Graves orbitopathy (GO), indicating that there might be regulators of the cytotoxicity of CD4 CTLs in GO [13]. Here, by analyzing RNA-sequencing (RNA-seq) data for PBMCs from patients with GO or Graves hyperthyroidism (GH), we identified the vascular endothelial growth factor (VEGF) A gene as a regulator of the cytotoxic function of CD4 CTLs in GO. Furthermore, single-cell RNA sequencing (scRNA-seq) and in vitro VEGF-A stimulation assay data analysis demonstrated that VEGF-A enhanced the cytotoxicity of pan CD4 CTLs. Mechanistically, we discovered that VEGF-A, via the VEGF-receptor (R)1/2 and AKT/mTOR pathway, enhanced the cytotoxic activity of CD4 CTLs. These findings suggest that VEGF-A contributes to the enhancement of the cytotoxic function of CD4 CTLs and may serve as a therapeutic target in disorders involving CD4 CTLs.

Material and methods

Study subjects

Twenty-seven treatment-naïve GO patients, 24 treatment-naïve GH patients, and 14 healthy controls (HCs) were enrolled in this study. Regarding those recruited samples from GO patients, 20 were used for RNA-sequencing, 4 were for in-vitro VEGF-A stimulation assays, 3 were for ELISA assays, 7 were for VEGF-R-related assays, and 5 were for phosphorylated molecules-related assays. The GO and GH patients were recruited from the Department of Endocrinology, The First Affiliated Hospital of Xi'an Jiaotong University. This study was approved by the Ethics Committee of the First Affiliated Hospital of Xi'an Jiaotong University. We obtained informed consent from each patient and HC after explaining the purpose of our study.

Primary $CD4^+$ T-cell isolation and culture

For primary $CD4^+$ T-cell isolation, PBMCs were acquired utilizing Ficoll Paque Plus (GE Healthcare, USA) gradient cell separation according to the manufacturer's instructions. Next, the $CD4^+$ T Cell Isolation Kit, human (Miltenyi Biotec, Germany) was utilized to isolate $CD4^+$ T cells. Then, the cells were resuspended at 1×10^6 cells/mL and cultured in advanced RPMI1640 medium (Gibco, USA) supplemented with 10% fetal bovine serum (FBS; Gibco), 1% 2-mercaptoethanol (2-ME; Gibco) and 1% penicillin–streptomycin (Gibco) in 48-well plates precoated with 2 μg/mL anti-human CD3 antibody (BioLegend, USA). For VEGF-R-related assays, after incubation with 5 μg/mL anti-VEGF-R1 antibody (R&D Systems, USA) and/or 10 μg/mL anti-VEGF-R2 antibody (Abcam, USA) for 1 h, $CD4^+$ T cells were treated with blank (CON) or 15 ng/mL VEGF-A (R&D Systems, USA) for 2 days respectively. GolgiPlug Protein Transport Inhibitor (BD Bioscience, USA) was administered for the last 6 h to detect the cytotoxic molecules. Regarding AKT/mTOR inhibition assays, $CD4^+$ T cells were treated with blank (CON), 15 ng/mL VEGF-A, VEGF-A + 10 μM MK-2206 2HCl (AKT inhibitor, MedChemExpress, USA), VEGF-A + 100 nM rapamycin (mTOR inhibitor, Selleck, China) or VEGF-A + 10 μM MK-2206 2HCl + 10 μM MHY1485 (mTOR activator, MedChemExpress, USA) for 2 days in

the presence of GolgiPlug Protein Transport Inhibitor for the last 6 h.

Flow cytometry

Cells were resuspended at a final concentration of 1×10^7 cells/mL in flow cytometry staining buffer (eBioscience, USA). After blocking with TruStain FcX PLUS (BioLegend), surface staining was performed at 4 °C for 30 min. For intracellular staining, a transcription factor buffer set (BD Bioscience) was used to fix and permeabilize cells according to the manufacturer's instructions, and the cells were then stained for intracellular molecules at 4 °C for 45 min. Stained cells were run on a Canto II (BD Bioscience) and analyzed using FlowJo software version 10.7.2 (TreeStar).

For phosphorylated protein analysis, cells were fixed with 4% cold PFA for 10 min at room temperature, permeabilized and blocked with PBS buffer containing 0.1% Triton X-100 and 2% BSA for 1 h at 4 °C. Next, the cells were stained with primary antibodies for 1.5 h at 4 °C, followed by incubation with secondary antibodies and antibodies targeting cell-surface markers for 30 min at 4 °C. PBS buffer containing 0.1% Triton X-100 and 0.5% BSA was utilized to wash the cells.

The following monoclonal antibodies were used: anti-human CD4, anti-killer cell lectin-like G1 (KLRG1), anti-human granzyme GrmB, anti-human GrmA, anti-human perforin (Prf), and anti-human neuropilin (NRP)-1 from BioLegend; polyclonal anti-human VEGF-R1 from R&D Systems; polyclonal anti-human VEGF-R2 and an anti-rabbit IgG (H+L) secondary antibody from Abcam; anti-phosphorylated (p)-AKT from Cell Signaling Technology; anti-p-mTOR and anti-p-S6 kinase (S6K) from eBioscience; and anti-goat IgG (H+L) from Proteintech.

Enzyme-linked immunosorbent assay (ELISA)

Plasma was collected from GO patients, GH patients, and HCs for ELISA analysis to quantify the concentration of VEGF-A. After dilution, plasma samples were added to an ELISA plate precoated with 2 μg/mL anti-VEGF capture antibody (R&D Systems) and incubated for 4 h at room temperature. Next, 0.25 μg/mL biotinylated anti-VEGF-165 (the most common isotype of VEGF-A in humans) affinity-purified antibody (R&D Systems) was added and incubated for 1 h at room temperature [14]. After incubation with an Av-HRP conjugate, TMB reagent was added, and the optical density (O.D.) for each well was read with a microplate reader (KHB, China) set to 450 nm.

Quantitative PCR (qPCR)

A MACS bead system (Miltenyi) was used to sort $CD4^+KLRG1^+$ and naïve $CD4^+$ T cells according to the manufacturer's guidelines. Sorted cells were confirmed to be > 85–95% pure. RNA used for reverse transcription was extracted from approximately 100,000–500,000 sorted $CD4^+KLRG1^+$ from GO patients and CON/MHY1485 (an mTOR activator)/VEGF-A-stimulated samples or HC naïve CD4+T cells using the Direct-zol RNA Microprep Kit (Zymo Research, USA). The Prime Script Master Mix Kit (Takara, Japan) was used to synthesize cDNA according to the manufacturer's protocol, followed by qPCR analysis (SYBR green; Takara). ACTB mRNA expression was utilized as the normalization control. The primers used are listed in Table 1.

RNA-seq and analysis

PBMC samples from 20 GO and 20 GH patients were subjected to RNA-seq as described in our previous study [15]. After quality control, the "DESeq2" R package was used to identify differentially expressed genes (DEGs) [16]. DEGs with a fold change ≥ 2 ($|\log_2 FC| > 1$) and a false discovery rate (FDR) < 0.05 were considered significant. A protein–protein interaction (PPI) network was constructed with data from the STRING database (https://string-db.org/) and visualized with Cytoscape (version 3.8.0) [17]. The R package "clusterProfiler" (version 4.0.5) was used to perform gene set enrichment analysis (GSEA) [18]. Gene sets in the Molecular Signatures Database (MSigDB) were selected

Table 1 Sequences of primers in qPCR

Gene symbol	Forward (5′-3′)	Reverse (5′-3′)
VEGFR1	TTTGCCTGAAATGGTGAGTAAGG	TGGTTTGCTTGAGCTGTGTTC
VEGFR2	GGCCCAATAATCAGAGTGGCA	CCAGTGTCATTTCCGATCACTTT
NRP1	GGCGCTTTTCGCAACGATAAA	TCGCATTTTTCACTTGGGTGAT
GZMB	CCCTGGGAAAACACTCACACA	GCACAACTCAATGGTACTGTCG
GZMK	GGTGTTCTGATTGATCCACAGT	TGTGCGCCTAAAACCACAGT
PRF1	GTGGGACAATAACAACCCCAT	TGGCATGATAGCGGAATTTTAGG
ACTB	GCCTCGCCTTTGCCGA	CCCACCATCACGCCCTGG

as the reference gene sets, and a P value < 0.01 was set as the threshold [19]. The RNA-seq data reported in this paper have been deposited in the OMIX, China National Center for Bioinformation / Beijing Institute of Genomics, Chinese Academy of Sciences (https://ngdc.cncb.ac.cn/omix: accession no.OMIX002526).

scRNA-seq data analysis

Three scRNA-seq datasets containing CD4 CTLs, GSE106543, GSE149652, and GSE179292, were obtained from the Gene Expression Omnibus (GEO) database [20–22]. The details for the 3 datasets are listed in Table 2. Our previous scRNA-seq dataset for $CD4^+$ T cells from GO patients (SRP226183) combined with the 3 scRNA-seq datasets were integrated for analysis by the "Seurat" R package via the canonical correlation analysis (CCA) method (version 4.0) [13, 23]. The DEGs were ranked by P value from smallest to largest. The top 20 significant genes for each cluster were selected for display in a heatmap. The "clusterprofiler" R package was utilized to perform GSEA [18]. Pseudotime trajectory analysis was conducted with the "monocle" R package (version 2.22.0) [24]. Single-sample (ss)GSEA was executed with the R package escape (version 1.4.0), and the results were visualized with the "dittoSeq" R package (version 1.6.0) [25].

Statistical analysis

Statistical analyses were performed with GraphPad Prism 9.3.1 (GraphPad Software) or R 4.1.2. After a normality test was performed, 2-group data were analyzed using Student's t test or the Mann–Whitney test. For multigroup data, one-way ANOVA was utilized. Data are presented as mean ± SEM. A P value < 0.05 was considered statistically significant.

Table 2 Details of scRNA-seq datasets analyzed

Dataset	Subject	Cell type	References
GSE106543	HC PBMC	T_{emra}	[20]
GSE149652	Bladder tumor/normal tissue	$CD4^+$ T cells	[21]
GSE179292	CRSwNP nasal polyp tissue	$CD4^+$ T cells & ILC2	[22]
SRP226183	GO/GH PBMC	$CD4^+$ T cells	[13]

HC Healthy controls, *PBMC* Peripheral blood mononuclear cells, T_{emra} Effector memory T cells re-expressing CD45RA, *CRSwNP* Chronic rhinosinusitis with nasal polyps, *ILC2* Group 2 innate lymphoid cells, *GO* Graves orbitopathy, *GH* Graves hyperthyroidism

Results

VEGF-A contributes to the enhanced cytotoxicity of CD4 CTLs in GO

In a prior work, we found that GO patients contained CD4 CTLs that expressed more cytotoxic molecules than those from GH patients [13]. To investigate the regulators of the cytotoxicity of CD4 CTLs, transcriptome sequencing was carried out on PBMCs from GO and GH patients. There were 476 upregulated genes and 94 downregulated genes detected (Fig. 1A). After PPI analysis of the DEGs, VEGFA was identified as a potential key gene in GO (Fig. 1B). Furthermore, in the GO patients with higher VEGFA expression, the cellular response to the calcium ion process was upregulated (Fig. 1C). Additionally, VEGF-A was shown to be elevated at the protein level in the plasma of GO patients compared to that of GH patients and HCs (Fig. 1D; $P = 0.0359$ and 0.0284). Considering that the calcium ion response is involved in the synthesis and release of cytotoxic molecules in T cells, we hypothesized that VEGF-A contributed to the increased cytotoxic function of CD4 CTLs in GO [26]. Reanalyzing scRNA-seq data for GO patients was performed to confirm this theory, and it was discovered that GO CD4 CTLs with greater levels of GZMB, PRF1, NKG7, and GZMK expression had upregulated VEGFR1 (Fig. 1E). Furthermore, GSEA results showed that cytotoxic granule, cytolysis, and cell killing processes were enriched in GO CD4 CTLs with upregulated VEGFR1 expression (Fig. 1F). In addition, the proportions of cells expressing cytotoxic molecules such as GrmB, GrmA, and Prf were significantly increased after administrating VEGF-A to $CD4^+$ T cells from GO patients (Fig. 1G; $P < 0.0001$, = 0.0286 and 0.0066, respectively). In this way, VEGF-A contributes to the enhanced cytotoxicity of CD4 CTLs in GO and can increase the production of cytotoxic molecules by these cells.

VEGF-A promotes the cytotoxic function of CD4 CTLs

Three scRNA-seq datasets containing enriched CD4 CTLs (effector memory T cells re-expressing CD45RA, Temra) or $CD4^+$ T cells were downloaded from the GEO database, and integrated analysis was performed with our previous scRNA-seq data (SRP226183) related to GO to further explore the role of VEGF-A in pan CD4 CTLs (Fig. 2A, Table 2). In total, 14 clusters were found (Fig. 2A). Among them, cluster 2, 6, 7, and 10 were recognized as CD4 CTLs due to the upregulated expression of cytotoxic molecules (Fig. 2B). In the HC and GO datasets (GSE106543 and SRP226183), CD4 CTLs with increased cytotoxicity (cluster 2 and 7) predominated, but these cells did not predominate in the bladder cancer or chronic rhinosinusitis with nasal polyps (CRSwNP)

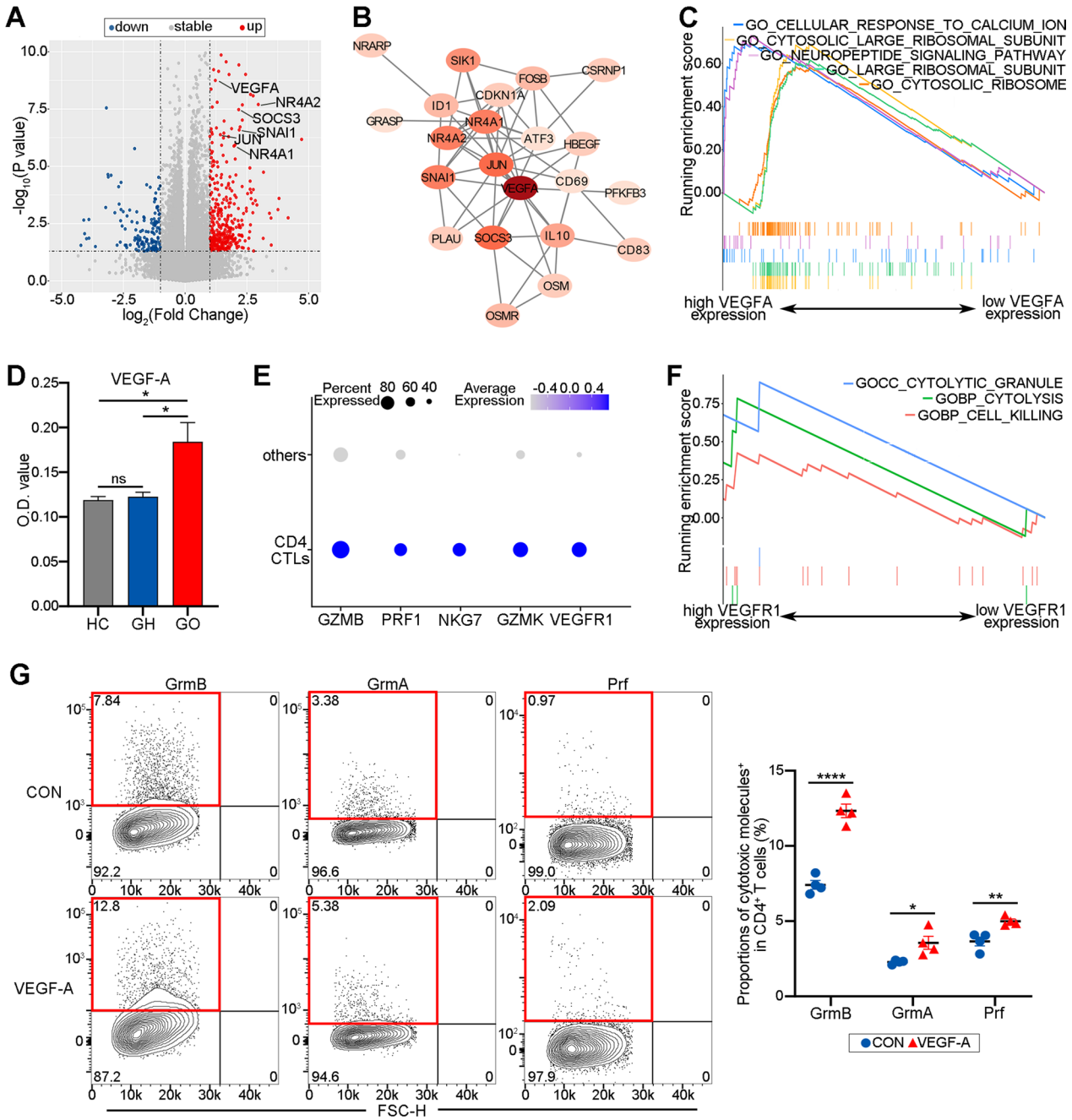

Fig. 1 VEGF-A contributes to the enhanced cytotoxicity of CD4 CTLs in GO. **A** Volcano plot showed differentially expressed genes between GO and GH group. Blue dots represented downregulated genes and red dots were upregulated genes. **B** PPI network of potential key genes. The shade of colors denoted the degree of the corresponding gene. **C** Gene set enrichment analysis (GSEA) showed cellular response to calcium ion process was obviously enriched in GO patients with higher expression of VEGFA compared with lower VEGFA expression. **D** Bar plot exhibited the O.D. value of VEGF-A in serum from HC, GH and GO patients (N = 3). **E** Dot plots showed the expression of GZMB, PRF1, NKG7, GZMK and VEGFR1 in CD4 CTLs and non-CD4 CTLs (other) group from GO patients respectively. Color scale represented *z*-score and dot size represented percentages of cells. **F** GSEA showed cytotoxic related processes were obviously enriched in CD4 CTLs from GO patients with higher expression of VEGFR1 compared with lower VEGFR1 expression. **G** Representative flow cytometry plots showed the ratios of $GrmB^+$, $GrmA^+$ and Prf^+ cells in $CD4^+$ T cells in the CON and VEGF-A group (N = 4). The red rectangle and number denoted in it meant $GrmB^+$, $GrmA^+$ and Prf^+ subsets and specific ratio respectively. The quantification of the proportions of $GrmB^+$, $GrmA^+$ and Prf^+ in $CD4^+$ T cells was displayed on the right. Blue was CON and red for VEGF-A treated. Error bars showed SEM. The data were representative of at least three biological replicates. HC: healthy control; GH: Graves hyperthyroidism; GO: Graves orbitopathy; CON: control; Grm: granzyme; Prf: perforin. $^*P < 0.05$, $^{**}P < 0.01$, $^{****}P < 0.0001$

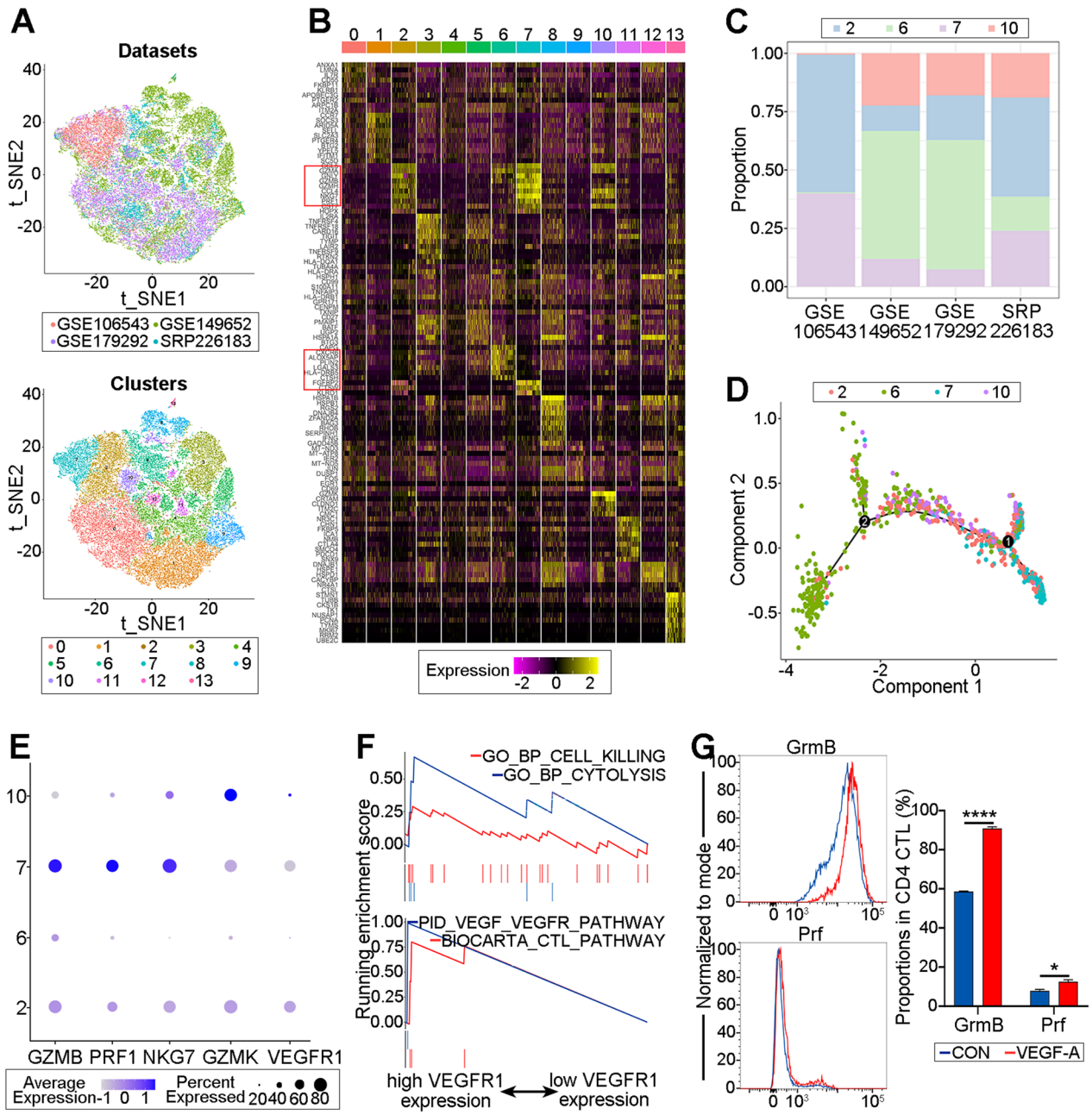

Fig. 2 VEGF-A promotes the cytotoxic function of CD4 CTLs. **A** The graph-based clustering and t-SNE algorithm were applied in $CD4^+$ T cells from GSE106543 (pink), GSE149652 (green), GSE179292 (purple) and SRP226183 (blue). Clusters denoted by the same color scheme were labeled with inferred cell types (bottom). **B** Heatmap from scRNA-seq analysis via expression data of the top 20 genes differentially expressed for each cluster (denoted by colored bars at the top). Key genes for each cell type were shown on the left margin. Genes in red rectangle represented cytotoxicity related. **C** The stack plots showed the ratio of each cluster of CD4 CTLs. Each color represented different cell cluster. **D** Pseudo-time trajectory analysis showed the differentiation stage of each CD4 CTLs subset according to the cytotoxicity. Pink represented cluster 2, green was cluster 6, blue was cluster 7 and purple was cluster 10. **E** Dot plots showed the expression of GZMB, PRF1, NKG7, GZMK and VEGFR1 in each CD4 CTLs subset respectively. Color scale represented z-score and dot size represented percentages of cells. **F** GSEA showed (upper) cytotoxic related processes and (bottom) VEGF and cytotoxicity pathways were obviously enriched in CD4 CTLs with higher expression of VEGFR1 compared with lower VEGFR1 expression. **G** Representative histogram plots showed the expression of GrmB and Prf in CD4 CTLs in the CON and VEGF-A group. The quantification of the proportions of $GrmB^+$ and Prf^+ in CD4 CTLs was displayed on the right (N = 3). Blue was CON and red for VEGF-A treated. Error bars showed SEM. The data were representative of at least three biological replicates. CON: control; Grm: granzyme; Prf: perforin. $^*P < 0.05$, $^{****}P < 0.0001$

datasets (GSE149652 and GSE179292; Fig. 2C&E). It was assumed that CD4 CTLs in lesions tended to be exhausted with decreased cytotoxicity given that pseudotime trajectory analysis suggested that cluster 6 and 10 might differ from cluster 2 and 7 (Fig. 2D; Additional file 1: Fig. S1). Notably, CD4 CTLs with greater cytotoxicity had upregulated VEGFR1 (clusters 2 and 7; Fig. 2E). Through GSEA, it was discovered that cluster 2 and 7, which had higher VEGFR1 expression, exhibited upregulation of processes related to VEGF_VEGFR signaling and cytotoxicity (Fig. 2F). Furthermore, in contrast to cells treated with the blank control, VEGF-A-treated CD4 CTLs from HCs produced more GrmB and Prf (CON; Fig. 2G; $P<0.0001$ and $P=0.0211$). These findings demonstrate that VEGF-A is involved in the cytotoxicity of CD4 CTLs and promotes their cytotoxic function.

VEGF-R1/R2 correlates with the cytotoxic function of CD4 CTLs

Although preliminary evidence suggests that VEGF-A regulates CD4 CTLs, the specific VEGF-R involved remains unknown. To clarify the downstream receptors, qPCR was performed to measure the expression of well-known VEGF-A receptors including VEGFR1, VEGFR2, and NRP1 on CD4 CTLs with increased cytotoxicity. Because GO $CD4^+$ T cells expressed much more cytotoxic molecules than those from HCs, GO CD4 CTLs were used as an example of CD4 CTLs with increased cytotoxicity (Additional file 2: Fig. S2; GrmB: $P=0.0083$; Prf: $P=0.0301$). The results revealed that VEGFR1 and VEGFR2 were upregulated in GO CD4 CTLs with increased cytotoxicity compared with HC naïve $CD4^+$ T cells (Fig. 3A; $P=0.0286$, 0.0409 and 0.4857, respectively). In contrast, there were lower proportions of VEGF-$R1^+$ and VEGF-$R2^+$ cells in GO CD4 CTLs with higher cytotoxicity than in HC CD4 CTLs, as measured by flow cytometry (Fig. 3B; VEGF-R1: $P=0.0001$; VEGF-R2: $P=0.0016$; NRP-1: $P=0.9240$). We hypothesized that the decrease in the level of VEGF-R1/R2 expression on GO CD4 CTLs with increased cytotoxicity was caused by binding with overexpressed VEGF-A because VEGF-R1/R2 levels were reported to be diminished following binding to VEGF [27]. As expected, GO CD4 CTLs with higher cytotoxicity had higher levels of phosphorylated (p)-VEGF-R2 than CD4 CTLs from HCs or GH patients (Fig. 3C; $P=0.0480$ and 0.0041), indicating that VEGF/VEGF-R2 signaling was upregulated in CD4 CTLs with enhanced cytotoxicity.

Furthermore, the relationships between the expression of VEGF-R1/R2 and cytotoxic molecules were examined. When VEGF-$R1^+$ GO CD4 CTLs with higher cytotoxicity were compared to VEGF-$R1^+$ HC CD4 CTLs, it was revealed that the proportions of $GrmB^+$ cells were increased, while no differences were detected between GO and HC CD4 CTLs with VEGF-$R1^-$ or VEGF-$R2^{\pm}$ (Fig. 3D&E; $P=0.0184$, 0.1594, 0.9745 and 0.7348). With respect to the proportion of Prf^+ cells, there were no differences between VEGF-$R1^+$ or VEGF-$R2^{\pm}$ GO and HC CD4 CTLs (Fig. 3D&E; $P=0.6380$, 0.1858, and 0.9856). Interestingly, VEGF-$R1^-$ GO CD4 CTLs had higher Prf expression than VEGF-$R1^-$ HC CD4 CTLs (Fig. 3D; $P=0.0230$). Hence, VEGF-R1/R2 signaling is upregulated in CD4 CTLs with increased cytotoxicity and correlated with higher cytotoxicity to some extent.

VEGF-A enhances the cytotoxic function of CD4 CTLs *via* VEGF-R1/R2

To identify the functional downstream receptors of VEGF-A in CD4 CTLs with increased cytotoxicity, $CD4^+$ T cells from GO patients were treated with anti-VEGF-R1/R2 neutralizing antibodies. After VEGF-R1 was blocked, the enhancement of GrmA and Prf production in CD4 CTLs induced by VEGF-A was suppressed (Fig. 4A, C, D; $P=0.0055$ and 0.0128). Furthermore, only the proportion of $GrmA^+$ cells in CD4 CTLs was diminished in the VEGF-A + anti-VEGF-R2 group compared to the VEGF-A group (Fig. 4A, C; $P=0.0450$). Additionally, the expression of GrmB, GrmA and Prf in CD4 CTLs was significantly decreased in the group with VEGF-R1 and VEGF-R2 blocked simultaneously in comparison to the VEGF-A group (Fig. 4A–D; $P=0.0283$, 0.0226 and 0.0468, respectively). These findings suggest that VEGF-A concurrently activates VEGF-R1 and VEGF-R2 to induce the production of cytotoxic molecules in CD4 CTLs.

AKT/mTOR signaling is upregulated in CD4 CTLs with increased cytotoxicity

The scRNA-seq data was used to further investigate downstream signaling through ssGSEA of the enriched pathways between CD4 CTLs with higher and lower cytotoxicity. In CD4 CTLs with enhanced cytotoxicity, the AKT pathway was upregulated in addition to the VEGF signaling pathway (Fig. 5A; $P<0.0001$). AKT signaling might be involved in the impact of VEGF-A-VEGF-R2 on CD4 CTLs with increased cytotoxicity, as evidenced by the MFI of p-AKT being considerably increased in GO CD4 CTLs with increased cytotoxicity, particularly in p-VEGF-$R2^+$ GO CD4 CTLs (Fig. 5B-C; $P=0.0006$ and 0.0290). In addition, the MFIs of p-mTOR and p-S6K were obviously elevated in CD4 CTLs with enhanced cytotoxicity (Fig. 5D–E; $P=0.0016$ and 0.0394), which indicated the activation of mTOR signaling. Therefore, the AKT/mTOR pathway may contribute to the effects of VEGF-A on CD4 CTLs with elevated cytotoxicity.

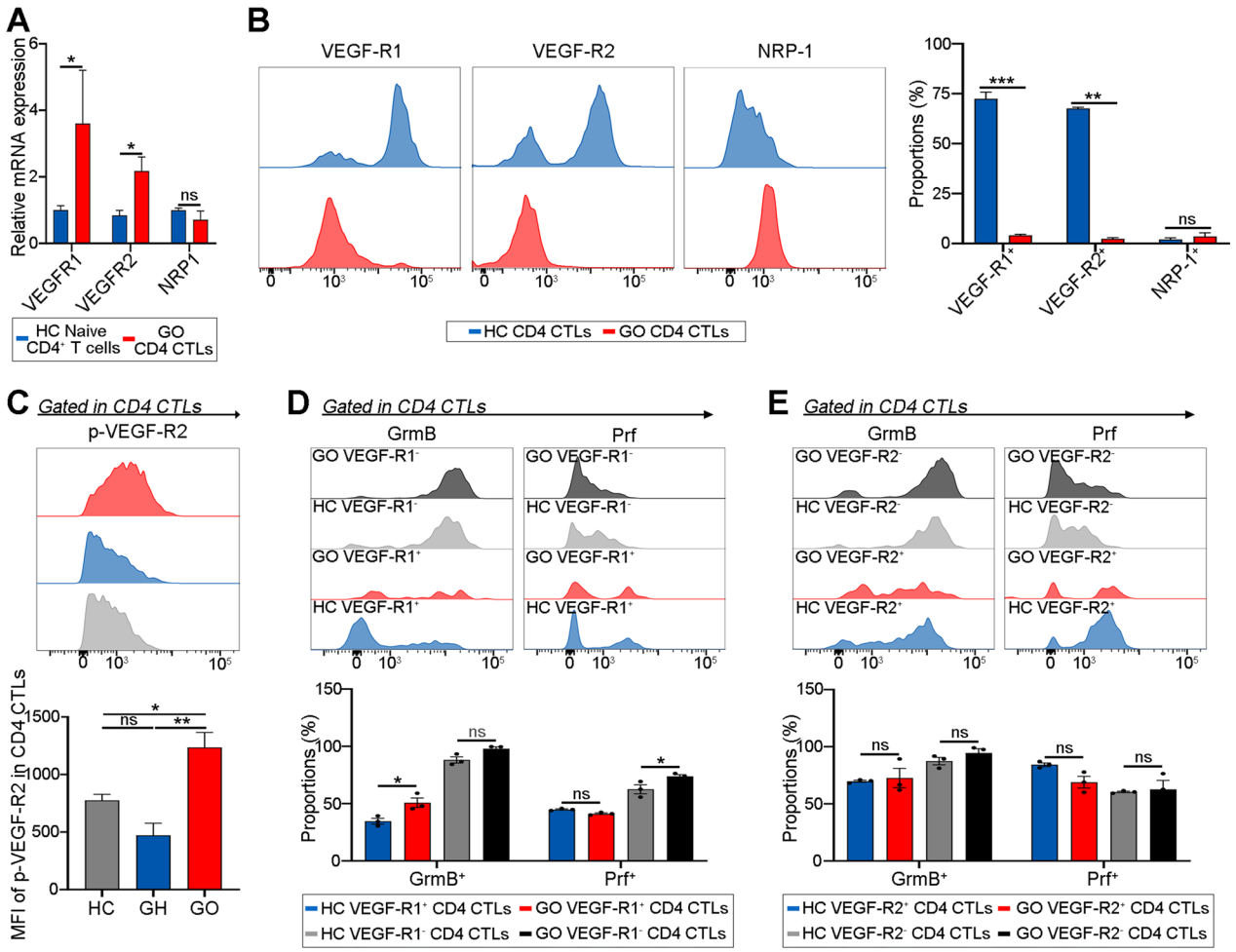

Fig. 3 VEGF-R1/R2 correlates with the cytotoxic function of CD4 CTLs. **A** Bar plots exhibited levels of VEGFR1, VEGFR2 and NRP1 in CD4 CTLs (red) from GO patients and $CD4^+$ Naive T cells (blue) from HC (N = 4). **B** Representative histogram plots exhibited the expression of VEGF-R1, VEGF-R2 and NRP-1 in CD4 CTLs from GO (red) and HC (blue) (N = 3). The bar plots showed the proportions of VEGF-$R1^+$, VEGF-$R2^+$ and NRP-1^+ cells in CD4 CTLs from GO (red) and HC (blue). **C** Representative histogram plots (upper) exhibited the expression of p-VEGF-R2 in CD4 CTLs from GO (red), GH (blue) and HC (gray) (N = 3). The bar plots (bottom) showed the MFI of p-VEGF-R2 in CD4 CTLs from GO (red), GH (blue) and HC (gray) group. **D**, **E** Representative histogram plots (upper) exhibited the expression of GrmB and Prf in (**D**) VEGF-R1/ (**E**) VEGF-R2 ±CD4 CTLs from GO (red and black) and HC (blue and gray) patients. The bar plots (bottom) showed the proportions of $GrmB^+$ and Prf^+ cells in (**D**) VEGF-R1/(**E**) VEGF-R2 ±CD4 CTLs from GO and HC group (N = 3). Blue denoted HC VEGF-$R1/2^+$ CD4 CTLs, red was GO VEGF-$R1/2^+$ CD4 CTLs, gray was HC VEGF-$R1/2^-$ CD4 CTLs and black was GO VEGF-$R1/2^-$ CD4 CTLs. Error bars showed SEM. The data were representative of at least three biological replicates. HC: healthy control; GH: Graves hyperthyroidism; GO: Graves orbitopathy; Grm: granzyme; Prf: perforin; p-VEGF-R2: phosphorylated VEGF-R2. *$P < 0.05$, **$P < 0.01$, ***$P < 0.001$

VEGF-A promotes the cytotoxic function of CD4 CTLs via *the AKT/mTOR pathway*

To determine whether the impacts of VEGF-A on CD4 CTLs were the cause of the activated AKT/mTOR signaling observed, the expression of p-AKT, p-mTOR and p-S6K was examined in CD4 CTLs treated with the blank control (CON) or VEGF-A. As anticipated, the MFIs of p-AKT, p-mTOR, and p-S6K were dramatically increased in the VEGF-A-treated CD4 CTLs (Fig. 6A; $P = 0.0460$, $P = 0.0344$ and 0.0047). In addition, at the gene expression level, there were obvious enhancements of GZMB, PRF1, and GZMK in the mTOR activator group compared with the CON group (Fig. 6D; $P = 0.0048$, 0.0010 and 0.0004 respectively). Moreover, after treating CD4 CTLs with an AKT inhibitor (MK-2206 2HCl) or mTOR inhibitor (rapamycin), the increases in the MFI of p-mTOR as well as the proportions of $GrmB^+$ and Prf^+ cells in CD4 CTLs induced by VEGF-A were significantly diminished, indicating that VEGF-A activates mTOR signaling via AKT and the facilitating effects of VEGF-A on the cytotoxicity of CD4 CTLs were achieved by AKT and mTOR signaling (Fig. 6E–H; AKT inhibitor: $P < 0.0001, < 0.0001$

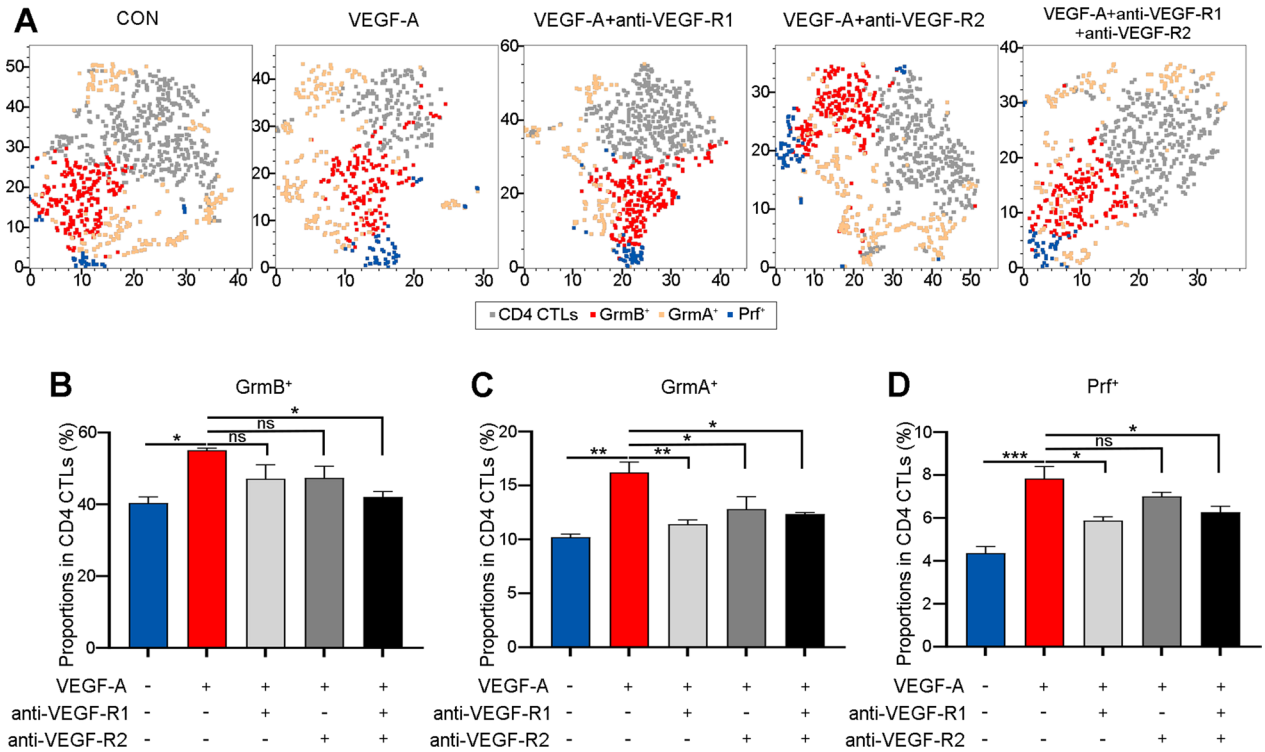

Fig. 4 VEGF-A enhances the cytotoxic function of CD4 CTLs via VEGF-R1/R2. **A** The representative tSNE plots showed the proportions of GrmB$^+$ (red), GrmA$^+$ (yellow) and Prf$^+$ (blue) in CD4 CTLs (gray). **B–D** The quantification of the ratio of **B** GrmB$^+$, **C** GrmA$^+$ and **D** Prf$^+$ cells in CD4 CTLs was shown in the bar plots (N = 3). Blue was CON, red for VEGF-A treated, light gray for VEGF-A + anti-VEGF-R1 neutralizing antibody, dark gray for VEGF-A + anti-VEGF-R2 neutralizing antibody and black for VEGF-A + anti-VEGF-R1 + anti-VEGF-R2 neutralizing antibody group. Error bars showed SEM. The data were representative of at least three biological replicates. CON: control; Grm: granzyme; Prf: perforin. *$P < 0.05$, **$P < 0.01$, ***$P < 0.001$

and = 0.0137; mTOR inhibitor: $P < 0.0001$, = 0.0002 and = 0.0140). Meanwhile, when an mTOR activator (MHY1485) was administered, the decrease in the MFI of p-mTOR as well as the proportions of GrmB$^+$ and Prf$^+$ cells in VEGF-A treated CD4 CTLs caused by the suppressed AKT could be rescued, implying the crucial role of mTOR in the downstream of AKT pathway in CD4 CTLs (Fig. 6E–H; P = 0.0296, < 0.0001 and = 0.0003). These results suggest that VEGF-A can enhance the cytotoxicity of CD4 CTLs via the AKT/mTOR pathway.

Discussion

In the current study, we identified that VEGF-A could induce the expression of cytotoxic molecules in CD4 CTLs via its receptors VEGF-R1/2 and this effect was achieved via the AKT/mTOR signaling pathway. These data reveal that VEGF-A is a regulator of the cytotoxicity of CD4 CTLs and provide insights for the development of novel treatments for disorders associated with CD4 CTLs.

VEGF-A, which is produced by the majority of cells, is a crucial member of the VEGF cytokine family, along with VEGF-B, VEGF-C, VEGF-D and placental growth factor (PIGF) [14]. Although its canonical biological function is angiogenesis mediated by regulating endothelial growth and vascular permeability, VEGF-A is also a mediator of T-cell function. When present in tumor-bearing individuals, VEGF-A has an immunosuppressive function that can inhibit the antitumor activity of CD8$^+$ T cells within tumors by aggravating the hypoxic microenvironment, activating an exhaustion-specific transcription program and prompting the proliferation and activity of regulatory T cells [28–30]. Furthermore, various effects of VEGF-A on T cells have been identified by several researchers. In combination with a cognate antigen, VEGF-A has been shown to trigger proinflammatory responses, including Th1, Th2 and Th17 activities, in vitro and/or in vivo (an asthma mouse model) [31–33]. Additionally, improved T-cell adhesion was observed in inflammatory bowel disease when high-dose VEGF-A was administered, which subsequently accelerated disease progression [34]. Notably, consistent with our findings that VEGF-A could enhance the cytotoxic function of CD4 CTLs (the majority of which exhibit a memory phenotype), VEGF has been shown to boost the immune responses of CD4$^+$CD45RO$^+$ memory T cells by upregulating the

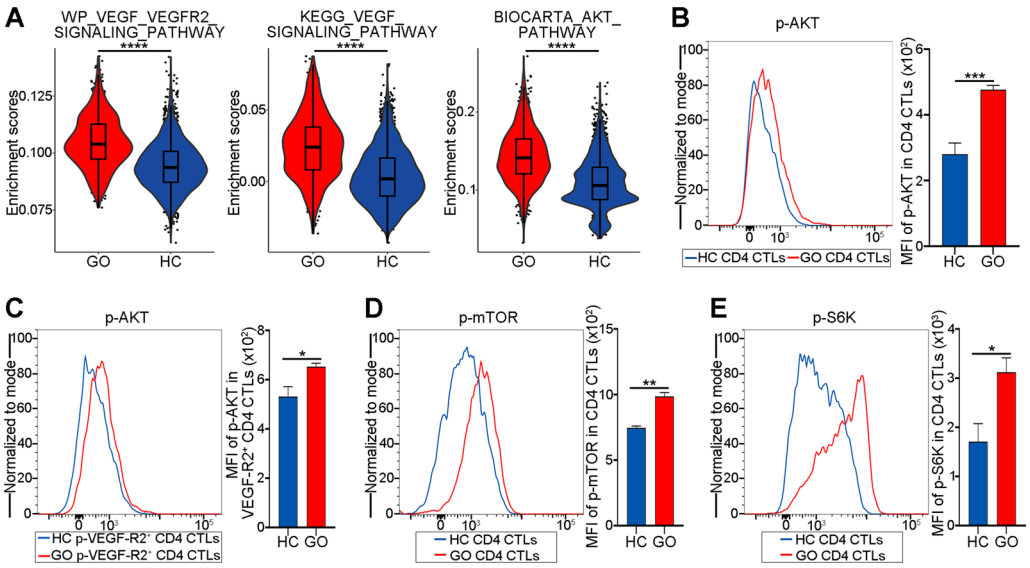

Fig. 5 AKT/mTOR signaling is up-regulated in CD4 CTLs with increased cytotoxicity. **A** Violin plots exhibited ssGSEA enrichment scores of VEGF signaling and AKT related pathways in CD4 CTLs from GO patients (red) and HC (blue). **B** Representative histogram plots (left) exhibited the expression of p-AKT in CD4 CTLs from GO (red) and HC (blue) (N = 5). The bar plots (right) showed the MFI of p-AKT in CD4 CTLs from GO (red) and HC (blue). **C** Representative histogram plots (left) exhibited the expression of p-AKT in p-VEGF-R2$^+$ CD4 CTLs from GO (red) and HC (blue) (N = 4). The bar plots (right) showed the MFI of p-AKT in p-VEGF-R2.$^+$ CD4 CTLs from GO (red) and HC (blue). **D**, **E** Representative histogram plots exhibited the expression of **D** p-mTOR and **E** p-S6K in CD4 CTLs from GO (red) and HC (blue) (N = 3). The bar plots showed the MFI of **D** p-mTOR and **E** p-S6K in CD4 CTLs from GO (red) and HC (blue). Error bars showed SEM. The data were representative of at least three biological replicates. ssGSEA: single sample gene score enrichment analysis; HC: healthy control; GO: Graves orbitopathy; mTOR: mammalian target of rapamycin; S6K: ribosomal protein S6 kinase. *$P < 0.05$, **$P < 0.01$, ***$P < 0.001$, ****$P < 0.0001$

phosphorylation and activation of extracellular signal-regulated kinase (ERK) and AKT [35]. Hence, VEGF-A is a pluripotent regulator that can enhance the cytotoxic function of CD4 CTLs.

Regarding VEGF-Rs, there are three major VEGF-A receptors: VEGF-R1, VEGF-R2 and NRP-1. Canonical VEGF signaling is transduced through VEGF-R1/R2, with VEGF-R2 being regarded as the dominant receptor, while NRP-1 is involved in increasing the binding affinity of VEGF-A for VEGF-R2 [14]. Previous studies have revealed that CD4$^+$ and CD8$^+$ T cells express VEGF-R1 and VEGF-R2 and that this expression increases significantly after T cells are activated [36]. The effects of VEGF-A on the aforementioned T cells are decreased after VEGF-R1/R2 are blocked, which is consistent with our results showing that both VEGF-R1 and VEGF-R2 contribute to VEGF-A signaling [37]. In addition, it was discovered that VEGF-R2 participates in the impacts of VEGF-A on natural killer (NK) cells, enhancing cytotoxic activity, which agrees with our results showing that VEGF-A enhances the cytotoxicity of CD4 CTLs via VEGF-R2 [38]. However, in this study, neutralizing antibodies were applied to block VEGF-Rs, and further investigation utilizing gene editing techniques in vitro and in vivo is needed. Additionally, the expression of VEGF-R1/R2 on the surface of CD4 CTLs with increased cytotoxicity was found to be reduced, while that of p-VEGF-R2 increased obviously, which implied the existence of ligand-activated endocytosis of VEGF-R2, as previously reported [27].

Given that AKT/mTOR signaling is a potential downstream cascade of VEGF stimulation, we identified the activation of the AKT/mTOR/S6K pathway in higher-cytotoxicity and VEGF-A-treated CD4 CTLs [39]. Application of the mTOR inhibitor rapamycin produced a reduction in the cytotoxicity of CD4 CTLs caused by VEGF-A, indicating that VEGF-A enhanced the cytotoxic function of CD4 CTLs via the mTOR pathway, which along with our findings that rapamycin could improve GO and suppress CD4 CTLs [40]. It has been reported that the antitumor immunity of CD8$^+$ T cells with defective AKT signaling diminished during the memory phase, and AKT cooperates with TCR- and IL-2- signaling to induce transcriptional processes controlling the expression of cytotoxic molecules in CTLs [41, 42]. Similarly, proteomic data for CTLs showed that mTORC1 preferentially repressed or promoted the expression of approximately 10% of CTL proteins [43]. Additionally, mTOR activation in CD8$^+$ T cells from rheumatoid arthritis patients was identified, and it was positively linked with the severity of the condition [44]. Therefore, AKT/mTOR signaling is involved

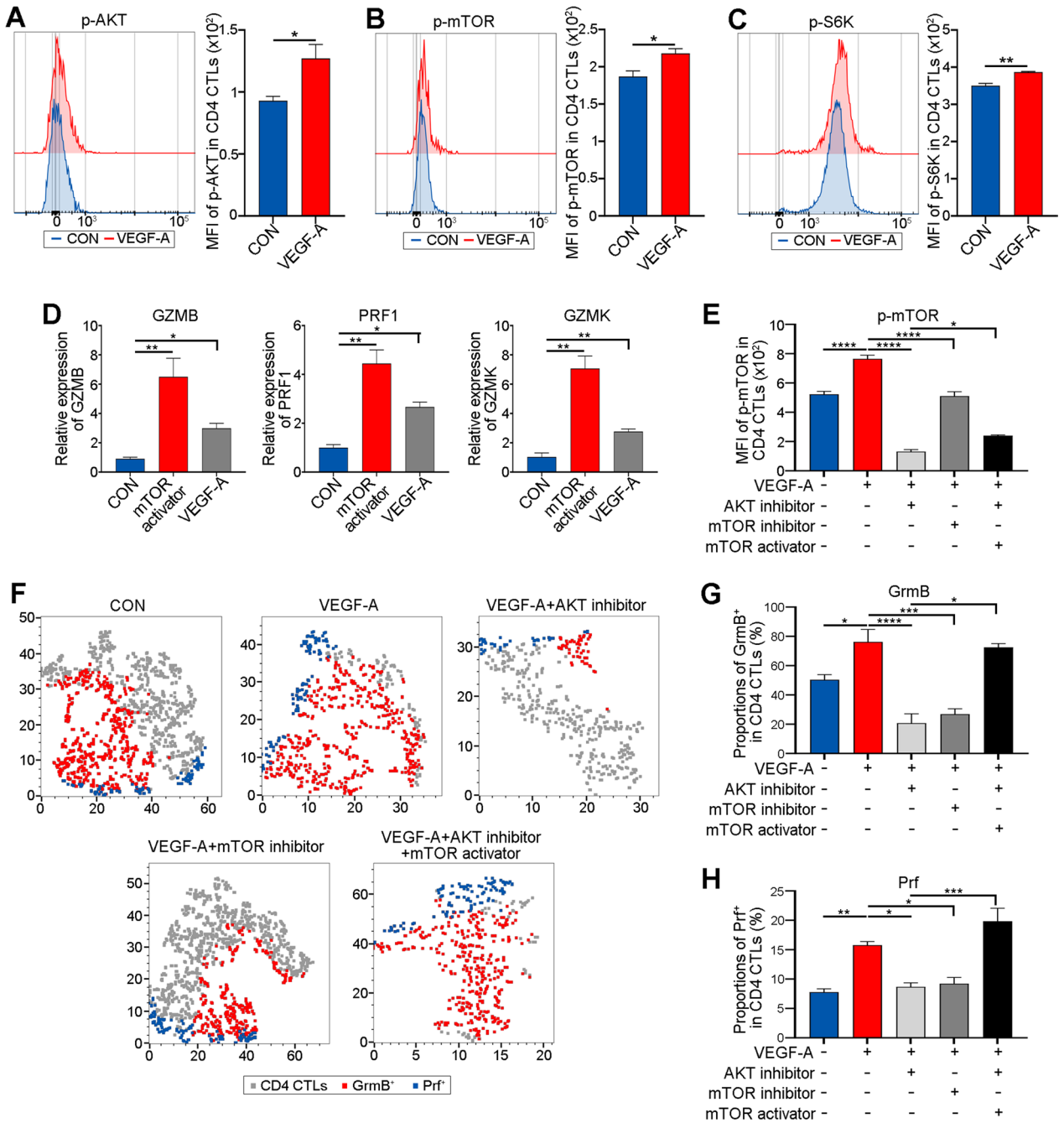

Fig. 6 VEGF-A promotes the cytotoxic function of CD4 CTLs via AKT/mTOR pathway. **A**, **B** Representative histogram plots (upper) exhibited the expression of **A** p-AKT **B** p-mTOR and **C** p-S6K in CD4 CTLs from CON (blue) and VEGF-A (red) group (N = 3). The bar plots (bottom) showed the MFI of **A** p-AKT **B** p-mTOR and **C** p-S6K in CD4 CTLs from CON (blue) and VEGF-A (red) group. **D** Bar plots exhibited levels of GZMB, PRF1 and GZMK in CD4 CTLs from CON (blue), mTOR activator (red) and VEGF-A (gray) group (N = 4). **E–H** The levels of **E** p-mTOR and **F–H** the proportions of $GrmB^+$ and Prf^+ in CD4 CTLs (N = 4). **F** The representative tSNE plots showed the proportions of $GrmB^+$ (red) and Prf^+ (blue) in CD4 CTLs (gray). The quantification of **E** the MFI of p-mTOR and ratio of **G** $GrmB^+$ and **H** $Prf.^+$ cells in CD4 CTLs was shown in the bar plots. Blue was CON, red for VEGF-A treated, light gray was VEGF-A + AKT inhibitor, dark gray for VEGF-A + mTOR inhibitor, and black was VEGF-A + AKT inhibitor + mTOR activator group. Error bars showed SEM. The data were representative of at least three biological replicates. CON: control; mTOR: mammalian target of rapamycin; Grm: granzyme; Prf: perforin. $^*P < 0.05$, $^{**}P < 0.01$, $^{***}P < 0.001$, $^{****}P < 0.0001$

in not only the cytotoxicity of CD8 CTLs but also that of CD4 CTLs.

Conclusions

In conclusion, VEGF-A promotes the cytotoxicity of CD4 CTLs via VEGF-R1/2, and this regulation is achieved by AKT/mTOR signaling. These data reveal that VEGF-A is a mediator of the cytotoxic function of CD4 CTLs and facilitate the development of novel treatments for disorders associated with CD4 CTLs.

Abbreviations

CD4 CTLs	$CD4^+$ cytotoxic T cells
MHC	Major histocompatibility complex
PBMCs	Peripheral blood mononuclear cells
TCR	T cell receptor
ThPok	T-helper-inducing POZ/Krueppel-like factor
Eomes	Eomesodermin
Grm	granzyme
IFN	Interferon
JAK	Janus kinase
STAT	Signal transducers and activators of transcription
GO	Graves orbitopathy
RNA-seq	RNA-sequencing
GH	Graves hyperthyroidism
VEGF	Vascular endothelial growth factor
scRNA-seq	Single-cell RNA sequencing
VEGF-R	VEGF-receptor
HCs	Healthy controls
CON	Control
KLRG1	Killer cell lectin-like G
Prf	Perforin
NRP	Neuropilin
p-	Phosphorylated
S6K	S6 kinase
DEGs	Differentially expressed genes
FC	Fold change
PPI	Protein–protein interaction
GSEA	Gene set enrichment analysis
GEO	Gene Expression Omnibus
CCA	Canonical correlation analysis
T_{emra}	Effector memory T cells re-expressing CD45RA
CRSwRP	Chronic rhinosinusitis with nasal polyps

Supplementary Information

The online version contains supplementary material available at https://doi.org/10.1186/s12967-023-03926-w.

Additional file 1: Fig. S1. The exhaustion signature was up-regulated in CD4 CTLs with lower cytotoxicity. A GSEA showed PD_1_SIGNALING was obviously enriched in CD4 CTLs with lower cytotoxicity compared with those with higher cytotoxicity ($P = 0.02192$). **B** Dot plots showed the expression of GZMB, PRF1, GZMA, PDCD1, LAG3, TIGIT and CTLA4 in CD4 CTLs with lower cytotoxicity and higher cytotoxicity respectively. Color scale represented z-score and dot size represented percentages of cells. **C** Pseudo-time trajectory analysis showed the expression of PDCD1, LAG3, TIGIT and CTLA4 in different differentiation stage of CD4 CTLs. Color scale represented log10(value + 0.1).

Additional file 2: Fig. S2. GO $CD4^+$ T cells had more cytotoxic molecules than those from HC. **A-B** Representative flow cytometry plots showed the ratios of **A** $GrmB^+$ and **B** Prf^+ cells in $CD4^+$ T cells in the GO and HC group (N = 3). The number denoted in it meant the specific ratio of $GrmB^+$ and Prf^+ subsets. The quantification of the proportions of **A** $GrmB^+$ and **B** Prf^+ in $CD4^+$ T cells was displayed in the bar plots. Blue was HC and red for GO. Error bars showed SEM. HC: healthy control; GO: Graves orbitopathy; Grm: granzyme; Prf: perforin. $^*P < 0.05$, $^{**}P < 0.01$.

Acknowledgements

We thank Mr. Xiaofei Wang at Biomedical Experimental Center of Xi'an Jiaotong University for his assistance with flow cytometry and bioinformatics analysis.

Author contributions

ZYC, MZ: Writing-original draft, Methodology, Formal analysis, Conceptualization; YFL: Methodology, Resources; ZC: Writing-review & editing; WJW, JCW: Investigation; MQH, LW: Software, Visualization; YW, BYS: Conceptualization, Funding acquisition, Supervision, Project administration, Validation, Writing-review & editing. All authors have read and approved the final version of this manuscript to be published. All authors read and approved the final manuscript.

Funding

This work was supported by National Natural Science Foundation of China (NSFC) (grant no. 82270827 (Y.W.), 82170805 (B.S.), 81970679 (B.S.), 82201238(M.Z.), the Young Star of Science and Technology in Shaanxi Province (grant no. 2022KJXX-56 (Y.W.)).

Availability of data and materials

Data supporting the findings of this study are available from the corresponding authors on reasonable request. The RNA-seq data have been deposited in the OMIX, China National Center for Bioinformation / Beijing Institute of Genomics, Chinese Academy of Sciences (https://ngdc.cncb.ac.cn/omix: Accession No.OMIX002526).

Declarations

Ethics approval and consent to participate

This study was approved by the Ethics Committee of the First Affiliated Hospital of Xi'an Jiaotong University. Informed consent was obtained from all individual participants after explaining the purpose of our study.

Consent for publication

Informed consent was obtained from all patients.

Competing Interests

The authors have declared that no conflict of interest exists.

Received: 16 December 2022 Accepted: 25 January 2023
Published online: 03 February 2023

References

1. Moretta L, Mingari MC, Sekaly PR, et al. Surface markers of cloned human T cells with various cytolytic activities. J Exp Med. 1981;154:569–74. https://doi.org/10.1084/jem.154.2.569.
2. Zaunders JJ, Dyer WB, Wang B, et al. Identification of circulating antigen-specific CD4+ T lymphocytes with a CCR5+, cytotoxic phenotype in an HIV-1 long-term nonprogressor and in CMV infection. Blood. 2004;103:2238–47. https://doi.org/10.1182/blood-2003-08-2765.
3. Hashimoto K, Kouno T, Ikawa T, et al. Single-cell transcriptomics reveals expansion of cytotoxic CD4 T cells in supercentenarians. Proc Natl Acad Sci USA. 2019;116:24242–51. https://doi.org/10.1073/pnas.1907883116.
4. Broux B, Pannemans K, Zhang X, et al. CX(3)CR1 drives cytotoxic CD4(+) CD28(-) T cells into the brain of multiple sclerosis patients. J Autoimmun. 2012;38:10–9. https://doi.org/10.1016/j.jaut.2011.11.006.
5. Jacquier A, Lambert T, Delattre JF, et al. Tumor infiltrating and peripheral CD4(+)ILT2(+) T cells are a cytotoxic subset selectively inhibited by HLA-G in clear cell renal cell carcinoma patients. Cancer Lett. 2021;519:105–16. https://doi.org/10.1016/j.canlet.2021.06.018.

6. Brown DM. Cytolytic CD4 cells: direct mediators in infectious disease and malignancy. Cell Immunol. 2010;262:89–95. https://doi.org/10.1016/j.cellimm.2010.02.008.
7. Mattoo H, Mahajan VS, Maehara T, et al. Clonal expansion of CD4(+) cytotoxic T lymphocytes in patients with IgG4-related disease. J Allergy Clin Immunol. 2016;138:825–38. https://doi.org/10.1016/j.jaci.2015.12.1330.
8. Mucida D, Husain MM, Muroi S, et al. Transcriptional reprogramming of mature $CD4^+$ helper T cells generates distinct MHC class II-restricted cytotoxic T lymphocytes. Nat Immunol. 2013;14:281–9. https://doi.org/10.1038/ni.2523.
9. Mittal P, Abblett R, Ryan JM, et al. An immunotherapeutic CD137 agonist releases eomesodermin from ThPOK repression in CD4 T cells. J Immunol. 2018;200:1513–26. https://doi.org/10.4049/jimmunol.1701039.
10. Chiu CY, Chang JJ, Dantanarayana AI, et al. Combination immune checkpoint blockade enhances IL-2 and CD107a production from HIV-specific T cells ex vivo in people living with HIV on antiretroviral therapy. J Immunol. 2022;208:54–62. https://doi.org/10.4049/jimmunol.2100367.
11. Ye W, Young JD, Liu CC. Interleukin-15 induces the expression of mRNAs of cytolytic mediators and augments cytotoxic activities in primary murine lymphocytes. Cell Immunol. 1996;174:54–62. https://doi.org/10.1006/cimm.1996.0293.
12. Barbosa CD, Canto FB, Gomes A, et al. Cytotoxic CD4(+) T cells driven by T-cell intrinsic IL-18R/MyD88 signaling predominantly infiltrate Trypanosoma cruzi-infected hearts. ELife. 2022. https://doi.org/10.7554/eLife.74636.
13. Wang Y, Chen Z, Wang T, et al. A novel CD4+ CTL subtype characterized by chemotaxis and inflammation is involved in the pathogenesis of Graves' orbitopathy. Cell Mol Immunol. 2021;18:735–45. https://doi.org/10.1038/s41423-020-00615-2.
14. Apte RS, Chen DS, Ferrara N. VEGF in signaling and disease: beyond discovery and development. Cell. 2019;176:1248–64. https://doi.org/10.1016/j.cell.2019.01.021.
15. Chen Z, Liu Y, Hu S, et al. Decreased treg cell and TCR expansion are involved in long-lasting Graves' disease Front. Endocrinol (Lausanne). 2021. https://doi.org/10.3389/fendo.2021.632492.
16. Love MI, Huber W, Anders S. Moderated estimation of fold change and dispersion for RNA-seq data with DESeq2. Genome Biol. 2014;15:550. https://doi.org/10.1186/s13059-014-0550-8.
17. Shannon P, Markiel A, Ozier O, et al. Cytoscape: a software environment for integrated models of biomolecular interaction networks. Genome Res. 2003;13:2498–504. https://doi.org/10.1101/gr.1239303.
18. Yu G, Wang LG, Han Y, et al. clusterProfiler: an R package for comparing biological themes among gene clusters. OMICS. 2012;16:284–7. https://doi.org/10.1089/omi.2011.0118.
19. Liberzon A, Birger C, Thorvaldsdóttir H, et al. The molecular signatures database (MSigDB) hallmark gene set collection. Cell Syst. 2015;1:417–25. https://doi.org/10.1016/j.cels.2015.12.004.
20. Patil VS, Madrigal A, Schmiedel BJ, et al. Precursors of human CD4(+) cytotoxic T lymphocytes identified by single-cell transcriptome analysis. Sci Immunol. 2018. https://doi.org/10.1126/sciimmunol.aan8664.
21. Oh DY, Kwek SS, Raju SS, et al. Intratumoral CD4(+) T cells mediate anti-tumor cytotoxicity in human bladder cancer. Cell. 2020;181:1612–25. https://doi.org/10.1016/j.cell.2020.05.017.
22. Ma J, Tibbitt CA, Georen SK, et al. Single-cell analysis pinpoints distinct populations of cytotoxic CD4(+) T cells and an IL-10(+)CD109(+) TH2 cell population in nasal polyps. Sci Immunol. 2021. https://doi.org/10.1126/sciimmunol.abg6356.
23. Satija R, Farrell JA, Gennert D, et al. Spatial reconstruction of single-cell gene expression data. Nat Biotechnol. 2015;33:495–502. https://doi.org/10.1038/nbt.3192.
24. Trapnell C, Cacchiarelli D, Grimsby J, et al. The dynamics and regulators of cell fate decisions are revealed by pseudotemporal ordering of single cells. Nat Biotechnol. 2014;32:381–6. https://doi.org/10.1038/nbt.2859.
25. Bunis DG, Andrews J, Fragiadakis GK, et al. dittoSeq: universal user-friendly single-cell and bulk RNA sequencing visualization toolkit. Bioinformatics. 2020;36:5535–6. https://doi.org/10.1093/bioinformatics/btaa1011.
26. Lyubchenko TA, Wurth GA, Zweifach A. Role of calcium influx in cytotoxic T lymphocyte lytic granule exocytosis during target cell killing. Immunity. 2001;15:847–59. https://doi.org/10.1016/s1074-7613(01)00233-3.
27. Simons M. An inside view: VEGF receptor trafficking and signaling. Physiology (Bethesda). 2012;27:213–22. https://doi.org/10.1152/physiol.00016.2012.
28. de Almeida PE, Mak J, Hernandez G, et al. Anti-VEGF treatment enhances CD8(+) T-cell antitumor activity by amplifying hypoxia, cancer. Immunol Res. 2020;8:806–18. https://doi.org/10.1158/2326-6066.CIR-19-0360.
29. Kim CG, Jang M, Kim Y, et al. VEGF-A drives TOX-dependent T cell exhaustion in anti-PD-1-resistant microsatellite stable colorectal cancers. Sci Immunol. 2019. https://doi.org/10.1126/sciimmunol.aay0555.
30. Tada Y, Togashi Y, Kotani D, et al. Targeting VEGFR2 with Ramucirumab strongly impacts effector/ activated regulatory T cells and CD8(+) T cells in the tumor microenvironment. J Immunother Cancer. 2018;6:106. https://doi.org/10.1186/s40425-018-0403-1.
31. Mor F, Quintana FJ, Cohen IR. Angiogenesis-inflammation cross-talk: vascular endothelial growth factor is secreted by activated T cells and induces Th1 polarization. J Immunol. 2004;172:4618–23. https://doi.org/10.4049/jimmunol.172.7.4618.
32. Kim YS, Choi SJ, Tae YM, et al. Distinct roles of vascular endothelial growth factor receptor-1- and receptor-2-mediated signaling in T cell priming and Th17 polarization to lipopolysaccharide-containing allergens in the lung. J Immunol. 2010;185:5648–55. https://doi.org/10.4049/jimmunol.1001713.
33. Kim YS, Hong SW, Choi JP, et al. Vascular endothelial growth factor is a key mediator in the development of T cell priming and its polarization to type 1 and type 17 T helper cells in the airways. J Immunol. 2009;183:5113–20. https://doi.org/10.4049/jimmunol.0901566.
34. Lee CG, Link H, Baluk P, et al. Vascular endothelial growth factor (VEGF) induces remodeling and enhances TH2-mediated sensitization and inflammation in the lung. Nat Med. 2004;10:1095–103. https://doi.org/10.1038/nm1105.
35. Goebel S, Huang M, Davis WC, et al. VEGF-A stimulation of leukocyte adhesion to colonic microvascular endothelium: implications for inflammatory bowel disease. Am J Physiol Gastrointest Liver Physiol. 2006;290:G648–54. https://doi.org/10.1152/ajpgi.00466.2005.
36. Basu A, Hoerning A, Datta D, et al. Cutting edge: Vascular endothelial growth factor-mediated signaling in human CD45RO+ CD4+ T cells promotes Akt and ERK activation and costimulates IFN-gamma production. J Immunol. 2010;184:545–9. https://doi.org/10.4049/jimmunol.0900397.
37. Rattanamahaphoom J, Leaungwutiwong P, Limkittikul K, et al. Activation of dengue virus-specific T cells modulates vascular endothelial growth factor receptor 2 expression. Asian Pac J Allergy Immunol. 2017;35:171–8. https://doi.org/10.12932/AP0810.
38. Cervi D, Shaked Y, Haeri M, et al. Enhanced natural-killer cell and erythropoietic activities in VEGF-A-overexpressing mice delay F-MuLV-induced erythroleukemia. Blood. 2007;109:2139–46. https://doi.org/10.1182/blood-2005-11-026823.
39. Sharma S, Guru SK, Manda S, et al. A marine sponge alkaloid derivative 4-chloro fascaplysin inhibits tumor growth and VEGF mediated angiogenesis by disrupting PI3K/Akt/mTOR signaling cascade. Chem Biol Interact. 2017;275:47–60. https://doi.org/10.1016/j.cbi.2017.07.017.
40. Zhang M, Chong KK, Chen ZY, et al. Rapamycin improves Graves' orbitopathy by suppressing CD4+ cytotoxic T lymphocytes. JCI Insight. 2022. https://doi.org/10.1172/jci.insight.160377.
41. Rogel A, Willoughby JE, Buchan SL, et al. Akt signaling is critical for memory CD8(+) T-cell development and tumor immune surveillance. Proc Natl Acad Sci U S A. 2017. https://doi.org/10.1073/pnas.1611299114.
42. Macintyre AN, Finlay D, Preston G, et al. Protein kinase B controls transcriptional programs that direct cytotoxic T cell fate but is dispensable for T cell metabolism. Immunity. 2011;34:224–36. https://doi.org/10.1016/j.immuni.2011.01.012.
43. Hukelmann JL, Anderson KE, Sinclair LV, et al. The cytotoxic T cell proteome and its shaping by the kinase mTOR. Nat Immunol. 2016;17:104–12. https://doi.org/10.1038/ni.3314.
44. Zhang M, Iwata S, Sonomoto K, et al. mTOR activation in CD8+ cells contributes to disease activity of rheumatoid arthritis and increases therapeutic response to TNF inhibitors. Rheumatology (Oxford). 2022;61:3010–22. https://doi.org/10.1093/rheumatology/keab834.

Publisher's Note